

African vulture optimizer algorithm for fuzzy logic speed controller of fuel cell electric vehicle

Basem E. Elnaghi¹, Mohammed Elshahat Dessouki^{2,3}, Sarah Wahied Mohamed¹, Ahmed M. Ismaiel¹,
Mohamed Nabil Abdel-Wahab¹

¹Department of Electrical Engineering, Faculty of Engineering, Suez Canal University, Ismailia, Egypt

²Department of Electrical Engineering, Faculty of Engineering, King Abdulaziz University, Rabigh, Saudi Arabia

³Department of Electrical Engineering, Faculty of Engineering, Port Said University, Port Said, Egypt

Article Info

Article history:

Received Sep 27, 2023

Revised Feb 24, 2024

Accepted Mar 1, 2024

Keywords:

African vulture optimizer
algorithm

Fuel cell electric vehicle

Fuzzy logic controller

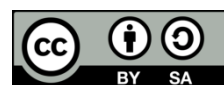
Genetic algorithm

Proton exchange membrane
fuel cell

ABSTRACT

This research article introduces a novel optimization strategy for fuel cell electric vehicles (FCEVs) in order to reduce the integral square error to enhance dynamic performance. African vulture optimizer algorithm (AVOA) improves a speed fuzzy logic controller's (FLC) internal controller settings. The AVOA is renowned for its simplicity in implementation, and low demand on computational resources. The speed drive of FCEV is investigated using MATLAB/Simulink 2023a. The results of FLC-AVOA provide lower settling time, lower overshoot, lower undershoot, and high dynamic response when compared to FLC and proportional-integral (PI) controllers designed using genetic algorithm (GA). The FLC-AVOA reduced the rising time for speed dynamic response by 2.31% and the maximum peak overshoot by 55.23% as compared to FLC-GA.

This is an open access article under the [CC BY-SA](https://creativecommons.org/licenses/by-sa/4.0/) license.



Corresponding Author:

Basem E. Elnaghi

Department of Electrical Engineering, Faculty of Engineering, Suez Canal University

El Sheikh Zayed, El Salam District, Ismailia 41511, Egypt

Email: Basem_elhady@eng.suez.edu.eg

1. INTRODUCTION

There are two fundamental issues with using fossil fuels, which provide 80% of the world's energy requirements. The scarcity of fossil fuels is the first issue; eventually, these resources will run out. According to petroleum company predictions, the extraction of fossil fuels, such as gasoline and natural gas, will peak in 2023 and then begin to decline. The second and most significant issue is that fossil fuels contribute significantly to critical environmental such as pollution, acid rain, global warming, and climate change. According to estimates, the annual cost of global environmental devastation is roughly \$5 trillion. The "Hydrogen fuel cell energy system" was first offered as a solution to the two worldwide issues in 1970. Hydrogen is a wonderful source of energy with many special features, as demonstrated over the past ten years by research and development activities carried out in universities and the laboratories of research organizations around the world. It is the most effective and pure fuel [1]. The research that eventually led to a functioning fuel cell began in the early 1800s, with Sir William Grove being recognized as its discoverer in 1839 [2].

The availability of energy affects a nation's economy, infrastructure, transportation, and quality of life. The discrepancy between global energy availability and use is an issue. All countries currently rely on non-sustainable sources of energy, namely fossil fuels, to provide their energy. To satisfy the world's energy demands, it is critical to transition to an alternate, sustainable energy source that is not harmful to the environment, which is expanding more quickly. Overall, there are many drawbacks to the current energy situation. Future generations will have far more hope if they use more of the several renewable energy sources

that already exist. Environmentalists believe that various actions will prevent the most likely outcome of global warming and its effects from occurring. Vehicles have improved in fuel efficiency over the past 20 years, and hybrid electric vehicles are becoming increasingly prevalent [3]. Fuel cells are completely clean power sources. The chemical energy in fuels is directly converted to electrical energy using fuel cells, which are electrochemical devices, offering the prospect of highly efficient and environmentally friendly power generation [4].

Fuel cells come in a variety of shapes and sizes, nevertheless, they all function by electrochemically combining fuel and oxygen to create heat, direct current electricity, and water. Anode, cathode, electrolyte, external electrical circuit, and fuel/air supply are the primary elements of a fuel cell. An oxygen-rich mixture is provided to the cathode, while fuel is delivered to the anode. The electrolyte's ion migration and the external circuit's electron flow together to produce the electrical current. "Systems" for fuel cells, which generally include one or more stacks, fuel reformers, fuel and air pre-heaters, afterburners, recycling routes, control systems, and power electronics, including DC-AC inverters, incorporate fuel cell "stacks," which are collections of various fuel cell "cells" [5]. Some forms of fuel cells include alkaline fuel cells, solid oxide fuel cells, proton exchange membrane fuel cells, and molten carbonate fuel battery types. Typically, low temperature fuels like alkaline fuel cell (AFC) and proton exchange membrane fuel cell (PEMFC), medium temperature fuels like phosphoric acid fuel cell (PAFC), and high temperature fuel cells like molten carbonate fuel cell (MCFC) and solid oxide fuel cell (SOFC), and AFC and PEMFC as other electrolyte fuel cells [6].

The most up-to-date research on drive/speed control techniques for electric motors is presented here. Electric electricity is transformed into mechanical power through the motor speed control. From fuel cells to electric motors, speed management is a complex topic that depends on approaches for smoothing drive controls via power electronic interface components. An interface component to achieve motor control in complete fuel cell electric vehicles (FCEVs) and hybrid FCEVs is an inverter that is linked between the electrical machine and the DC bus. The inverter makes it possible to regulate motors at different voltage and frequency levels. As noted in the marketing, brushless direct current (BLDC), synchronous, and induction motors are typically preferred in FCEVs. Similar inverter topologies can be utilized to control these motors. Utilizing inverters connected to electrical machines, speed control is accomplished. Their control algorithms, though, might be different from one another. The control algorithm for an electric motor can either be a conventional proportional integral derivative (PID) control or a very effective adaptive, fuzzy, or artificial neural network (ANN) control. Selecting the best motor control technique for FCEVs requires special consideration [7], [8]. Controlling the electric motor (EM)'s rotating direction, speed, acceleration, and torque is the main responsibility of the interface inverter element [9]. Different control techniques are used in FCEVs' AC/DC motors to achieve this control. Scalar or vector control for AC motors, and pulse width modulation (PWM) control for DC motors, is typically used to achieve motor control [10], [11].

DC motors in FCEVs can be either brushed or brushless. Brushed DC motors are the first type of DC motors used in FCEVs. Depending on the application, in this kind of motor, the stator's windings take the place of permanent magnets. However, this motor type is no longer used in modern commercial EVs [12], [13]. The BLDC motor used in FCEVs is a kind of DC motor that is comparable to an AC motor. Because the brush component is not connected to the armature, this motor's operating principle is also comparable to that of the permanent magnet synchronous motor (PMSM). The circumstance that separates the PMSM with an AC supply from the BLDC motor. Recently, there has been increased interest in using BLDC motors with EVs. Like PMSM, BLDC features is good motor control, great efficiency, and minimal volume. In order to further save costs, numerous sensors less commutation schemes have been proposed. However, this type of motor is still more expensive than induction motors [10]. Brushed DC motor drives and permanent magnet BLDC motor drives are the two primary categories of DC motor drives. Compared to AC motor drives, DC motor drives are easier to use and less expensive. With fuzzy logic, PI, and fuzzy logic-based self-tuning PI controllers, the motor control is explored.

On the other hand, because to their great efficiency and power density, In FCEVs, BLDC motors are commonly preferred. Additionally, because BLDC motors have magnetic poles, motor drives can be more efficient than other types of motor drives. Similar to this, the three-phase BLDC motor drive control can be controlled using the inverter architecture utilized with induction motor (IM). A BLDC motor's speed is managed using a fractional-order PI (FOPI) controller. When compared to the traditional PI approach, this controller is tracking more effectively. The moth swarm algorithm is used to obtain the FOPI controller's parameters. Furthermore, multiphase BLDC motors may use either a five-phase or seven-phase VSI. On the other hand, the BLDC motor's drive control algorithm should be fault-tolerant through the detection, identification, and recovery of the defect.

Recent work also mentions improved drive control for BLDC motors, similar to AC motor drives. Some of these researches seek to create a control algorithm by minimizing certain elements, like the quantity of sensors. For high-speed BLDC motors, the reverse electromotive force of the virtual third harmonic enables sensor-less drive control. This technique provides the rotor location and corrects for commutation mistake. The

current waveform-based approach decreases the torque ripple and commutation inaccuracy. Using this technique, switching ripple components are 33% lower [10], [14], [15].

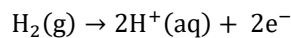
The PI Controller may make the steady-state error equal zero since it has an integral and proportional term in the forward path. In regions where the system velocity is on a big scale, PI controllers are used. The K_i part merely eliminates the steady-state error whereas the K_p part reduces the rise time, which may be done at the expense of the transient response. PI controller is primarily utilized in typical DC motor applications [16]. In August 2021, Abdollahzadeh *et al.* [17] proposed the African vulture optimization algorithm (AVOA), an entirely new metaheuristic algorithm inspired by nature. Its systems for exploration and exploitation are more inclusive. The use of a random technique improves both mechanisms' capacities for exploration and exploitation. This strategy can guarantee that the AVOA won't be very divergent, that it will skip a local optimum, and that it will converge rapidly [18]. It is necessary to properly construct the fuzzy logic speed controller for speed performance increase [19]. The main contribution of this article can be summarized as: i) Modelling and simulation of fuel cell electric vehicles; ii) Investigating the robustness of using fuzzy logic controller's (FLC) based on AVOA in fuel cell electric vehicles; and iii) Compare the FLC-AVOA with FLC-GA and PI-GA.

2. METHOD

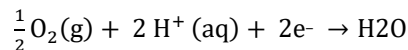
2.1. Fuel cell modelling

The most important part of an automotive fuel cell system is the fuel cell stack. As seen in Figure 1 and (1), it is in charge of generating DC current from the electrochemical activities taking place inside the fuel cell. Since a single fuel cell provides less than 1 voltage, many fuel cells must be stacked in series to meet the requirements of each potential application. The size of the fuel cell, operating temperature, fuel type, intake gas pressure, and other factors all have an impact on the stack's capacity. As an illustration, Toyota's Mirai fuel cell stack is presently one of the most innovative and creative in the business. The brand-new 2016 Mirai features 370 series-connected cells, a volume power density of 3.1 kW/L, and an external maximum electric output of 144 kW [20], [21].

At anode:



At cathode:



Overall reaction:

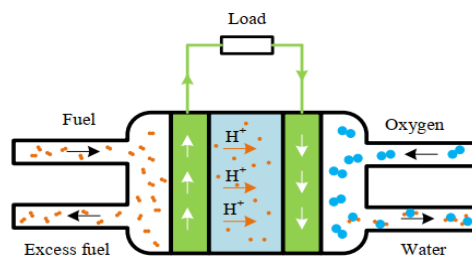
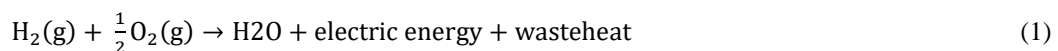


Figure 1. Proton exchange membrane fuel cell

The Nernst equation can be used to obtain the result voltage for a standard PEMFC fuel cell in order to determine the fuel cell's reversible potential. The behavior described by this equation only applies to a single fuel cell. The (2) will power each fuel cell in the fuel cell stack:

$$E_{\text{cell}} = E_{0,\text{cell}} + \frac{RT}{2F} \cdot \ln \left(\frac{P_{\text{H}_2} \cdot P_{\text{O}_2}^{0.5}}{P_{\text{H}_2\text{O}}} \right) \quad (2)$$

Assuming that the result of H₂O is liquid, the potential in fuel cell cars that use a traditional fuel source is shown in (3).

$$E_{\text{cell}} = E_{0,\text{cell}} + \frac{RT}{2F} \cdot \ln (P_{\text{H}_2} \cdot P_{\text{O}_2}^{0.5}) \quad (3)$$

$E_{0,\text{cell}}$ refers to the potential of the reference basis; this potential is also temperature-dependent as shown in (4).

$$E_{0,\text{cell}} = E_{0,\text{cell}}^0 - K_e \cdot (T - 298) \quad (4)$$

Where $E_{0,\text{cell}}$ stand for the typical reference cell potential (at 1 atmosphere, 25 degrees Celsius). Additionally, k_e is a constant that is derived empirically and represents the gain when $E_{0,\text{cell}}$ is calculated in (°K)⁻¹ units.

Considering that this is a PEMFC's internal output voltage, a number of voltage dips and effects must be taken into account. For instance, several delays in the fuel and oxidants may be described by the Laplace domain in (5).

$$E_{d,\text{cell}}(S) = \lambda_e \cdot I(S) \frac{T_e \cdot S}{T_e + 1} \quad (5)$$

A few voltage drops must be taken into account in addition to the impact of the fuel and oxidant delays. A PEMFC voltage output function will take into consideration the voltage dips stated in (6).

$$V_{\text{cell}} = E_{\text{cell}} - V_{\text{act,cell}} - V_{\text{ohm,cell}} - V_{\text{conc,cell}} \quad (6)$$

Where $V_{\text{act,cell}}$ represents activation voltage drop (activation losses), $V_{\text{ohm,cell}}$ represents ohmic voltage drop (ohmic losses), and $V_{\text{conc,cell}}$ represents concentration voltage drop (concentration losses) [20], [22]. The PEMFC from Toyota's Mirai company used in this research is illustrated in Table 1.

Table 1. Toyota's Mirai fuel cell stack – 144 KW -24 voltage specification model

Symbol	Nomenclature	Value
R_S	Internal resistance of the stack (Ohm)	0.06187 Ω
$I_{\text{FC,nom}}$	Nominal (rated) current of the stack (Amp)	52 A
$V_{\text{FC,nom}}$	Nominal (rated) voltage of the stack (volt)	24 V
$E_{o.c.}$	Cell open circuit voltage (volt)	1 V
$E_{o.c.}$	Stack open circuit voltage (volt)	42 V
E_n	Cell Nernst voltage	1.12 V
K_c	Voltage constant at nominal conditions	0.9
A	Tafel Slope	0.045885
N	Number of series cells in the stack	370 cells
I_0	Exchange current (Amp)	0.02732 A
V_{Fuel}	Volume of the fuel (m ³)	10 m ³
n	Number of moles	541
Δh°	Enthalpy change (Joule/mole)	241830
P_{Fuel}	Fuel pressure (bar)	1.5 bar
P_{Air}	Air pressure (bar)	1 bar
R	Gas constant (J/mole.K)	8.3145
T	Operating system temperature (K)	338 K
Q_{Fuel}	Fuel flow rate (litre/min)	12.2
Q_{Air}	Air flow rate (litre/min)	2400
Z	Number of moving electrons	4
P_{H_2}	Hydrogen pressure (bar)	1.64*10 ⁻³
P_{O_2}	Oxygen pressure (bar)	0.206
$P_{\text{H}_2\text{O}}$	Water pressure (bar)	
F	Faraday's constant a.sec/mole	96485
ΔG	Gibbs energy (Joule/mole)	133104.5
V_{-1}	Voltage at current of one ampere (volt)	35 V
K_G	Gibbs constant	0.61586
K	Boltzman constant J/K	1.38*10 ⁻²³
h	Plank constant (J.sec)	6.626* 10 ⁻³⁴
$Q_{\text{Air,max}}$	Maximum flow rate (lpm)	4800
X	Rated percentage of hydrogen in the fuel (%)	99.95
Y	Rated percentage of oxygen in the oxidant (%)	21
W	Rated percentage of water vapor in oxidant (%)	1
α	Exchange coefficient	0.308

2.2. DC/DC boost converter

This converter that raises a voltage input's value is a DC boost converter as shown in Figure 2. In the majority of cases, it raises the battery or fuel cell stack's direct current output voltage to 650 V when the high voltage (HV) components need it. This implies that the same current can be used to generate greater power. Another advantage of having greater power is the ability to reduce the number of fuel cells per stack and the quantity of cells in the battery pack. This affects the weight and ultimately the fuel cell vehicles (FCV's) overall performance [20].

As illustrated in Figure 3, when operating in discontinuous mode, the inductor can finish discharging before the switching cycle is finished. The voltage adjustment that affects the boost converter's switch duty cycle can be used to get a correct output set to 650 V. The required reference voltage is compared to the output voltage [5], [20].

With the right PID controller, we can compute and correct output voltage error, allowing us to acquire the signal for control. Once the signal for control has been received, it may be used to adjust the duty cycle higher or lower until the voltage output approaches the desired voltage reference by comparing it to a reference saw tooth signal. Understanding the needed input and output voltage ranges, and desired power transfer allows one to compute the converter's design parameters. The highest possible duty cycle ratio is calculated as in (7).

$$D_{MAX} = 1 - \frac{V_{inMIN} \cdot \eta_{converter}}{V_{out}} \tag{7}$$

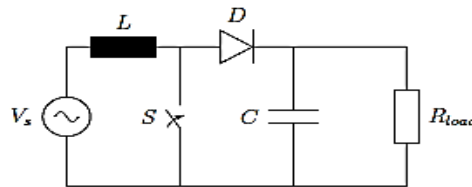


Figure 2. Circuit of boost converter for DC/DC

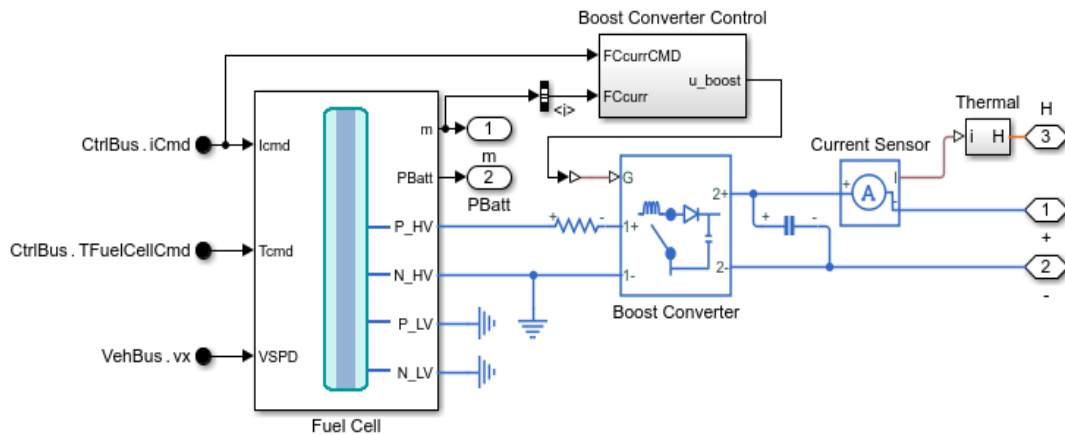


Figure 3. DC/DC boost converter control model

2.3. African vulture optimizer algorithm

AVOA approach is divided into four stages based on the aforementioned four requirements in order to mimic the behavior of various vultures during the foraging stage.

a. Population grouping

The best answer is selected as the best and first vulture in this stage, the second solution is selected as the second-best vulture, and the other vultures are grouped together into a third group according to the second criterion. This phase comes after the initial population is formed in (8) [18].

$$R(i) = \begin{cases} BV_1 & \text{if } p_i = Z_1 \\ BV_2 & \text{if } p_i = Z_2 \end{cases} \tag{8}$$

Where, Z_1 and Z_2 are two random values in the range of $[0,1]$, BV_1 , and BV_2 represent the first and second-best vulture, and their total is 1. p_i is done with the roulette-wheel method.

b. Exploration stage

Vultures can quickly find food and recognize dead animals because of their superior environmental perception. However, vultures may have problems locating food since they spend a lot of time examining their surroundings before traveling huge distances in quest of it. Vultures in the AVOA can inspect various random locations using two distinct strategies, and a parameter named P_1 in the range of $[0, 1]$ is used to get either strategy.

To choose one of the strategies during the exploration phase, a random number $rand_{p_1}$ between 0 and 1 is utilized. (9) is used if the value of $rand_i \leq P_1$, otherwise (10) is employed.

$$P(i + 1) = R(i) - D(i) \times F_i \quad (9)$$

$$P(i + 1) = R(i) - F_i + rand_2 \times ((ub - lb) \times rand_3 + lb) \quad (10)$$

Where, $R(i)$ stands for one of the best vultures chosen in the current iteration with (8). $rand_2$ is a random number between 0 and 1, and lb and ub are the variables' lower and upper bounds, respectively. To increase the variety and search for different search space areas, $rand_3$ is used to give a high random coefficient at the search environment scale.

c. Exploitation

The efficiency stage of the AVOA is currently being studied in (11). First, the AVOA initiates the exploitation phase. If $|F_i| < 1$. Then $P_2 \in [0,1]$ is used to decide which method is selected. $rand_{p_2}$ is a random number between 0 and 1 produced. The siege-fight strategy is applied slowly if this $rand_{p_2} \geq P_2$.

$$P(i + 1) = \begin{cases} D(i) \times (F_i + rand_4) - d(t) & \text{if } P_2 \geq rand_{p_2} \\ R(i) - S_1 - S_2 & \text{if } P_2 < rand_{p_2} \end{cases} \quad (11)$$

d. Exploitation

If $|F_i|$ is smaller than 0.5. $rand_3$ is a random number between 0 and 1. So if $P_3 \geq rand_3$. The idea behind the technique is to entice several vulture species to gather around the food source and start a competition. This means that the location of the vulture may be updated using (12).

$$P(i + 1) = \frac{A_1 + A_2}{2} \quad (12)$$

Where, A_1 and A_2 are given by (13) and (14).

$$A_1 = BV_1(i) - \frac{BV_1(i) \times P(i)}{BV_1(i) - (P(i))^2} \times F_i \quad (13)$$

$$A_2 = BV_2(i) - \frac{BV_2(i) \times P(i)}{BV_2(i) - (P(i))^2} \times F_i \quad (14)$$

2.4. Speed controller

2.4.1. PI controller

For this strategy, the control law is show in (15) and (16).

$$T = K_p * e + K_i * \int e dt \quad (15)$$

$$e = \omega^* - \omega \quad (16)$$

Where ω and ω^* are, respectively, the actual and reference speed. The PI speed regulator gains control the controller's output (K_p and K_i) that follow a set of criteria to provide the greatest control performance feasible even in the face of parameter volatility and drive nonlinearity, as shown in Figure 4. The high value of the error is amplified across the PI regulator in beginning mode, leading to substantial differences in the required torque. If the K_p and K_i Overcoming a certain threshold causes the needed torque to fluctuate too much, which causes the system to become unstable. After the PI regulator, a limiter is utilized to address this issue. When calibrated correctly, this limiter maintains the speed inaccuracy within boundaries, resulting in smooth swings in the required torque even when the PI speed regulator improvements are rather substantial. The K_p and K_i values of the PI speed regulator's efficiency has been calculated using genetic algorithm (GA) [23], [24].

2.4.2. Fuzzy logic controller

The fuzzy logic controller method is found to be significantly more effective. When creating the regulator, nonlinearization takes into account the person's skill and expertise in the process that has to be controlled. The performance, dependability, and resilience of the system are enhanced when using this approach as opposed to conventional linear regulators. Gain coefficients K_p , K_d , and K_o illustrated in Figure 5 are used in the model, and they are set to 30, 40, and 100, respectively. These coefficients were calculated using AVOA. A Sugeno-type fuzzy inference systems (FIS) with two inputs is used to simulate the regulator model the error "e", the change in error " Δe " and one output (T_{e^*}) [22], [25].

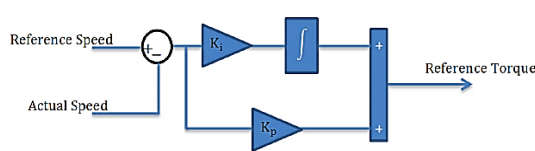


Figure 4. PI controller scheme

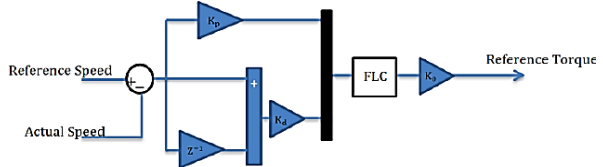


Figure 5. FLC scheme

3. SYSTEM SETUP

The system setup model of fuel cell electric vehicle is illustrated in Figure 6. The fuel cell is supplying unidirectional DC/DC converter which is coupled to motor controller. The fuel cell is powering motor controller through DC/DC converter. The motor controller is achieved using FLC-AVOA, FLC-GA, and PI-GA.

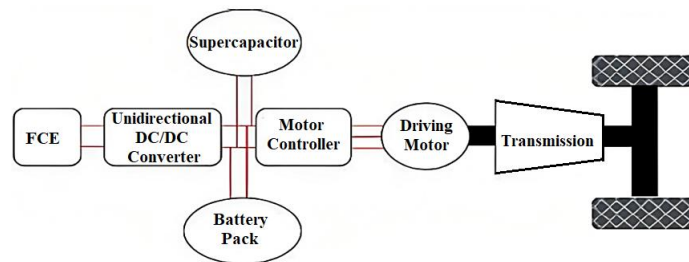


Figure 6. System model setup

4. RESULTS AND DISCUSSION

To evaluate the performance of the speed controller-based energy management strategy, the electric car powered by a fuel cell model has been implemented and simulated in MATLAB/Simulink, the result of the simulation. In Figure 7 it is observed that the overshoot peak value of motor speed employing fuzzy logic controller with AVOA is less than in fuzzy logic control using GA and PI control using GA, and the rising time of AVOA-based fuzzy logic control is lower than that of other methods. In the FLC-AVOA reduced the rising time for speed dynamic response by 2.31% and the maximum peak overshoot by 55.23% as compared to FLC-GA.

In Figure 8 shows that using fuzzy logic controller with AVOA in fuel cells power has better response than using fuzzy logic control with Ga and PI control with GA, and fuzzy logic control using AVOA has less rising time than others. Figure 9 displays the output motor torque generated when simulating various control strategies. It is found that, in contrast to PI and Fuzzy with GA, the fuzzy logic controller with AVOA has a very low steady state torque ripple and lowers the transient peak torque.

In Figure 10, it is noted that the output fuel cell voltage produced under the simulation, the fuzzy logic controller with AVOA shows less rising time so it is better than in PI and fuzzy with GA. From the results we find that these methods include the proportional integral controller, fuzzy logic controller, modified fuzzy controller technique using African vulture optimizer algorithms, and genetic algorithm. For power management in the FCEV, fuzzy control using African vulture optimizer algorithms has been suggested. The outcomes of the simulation show that the proposed strategy is appropriate for this system and that the desired level of power management is attained.

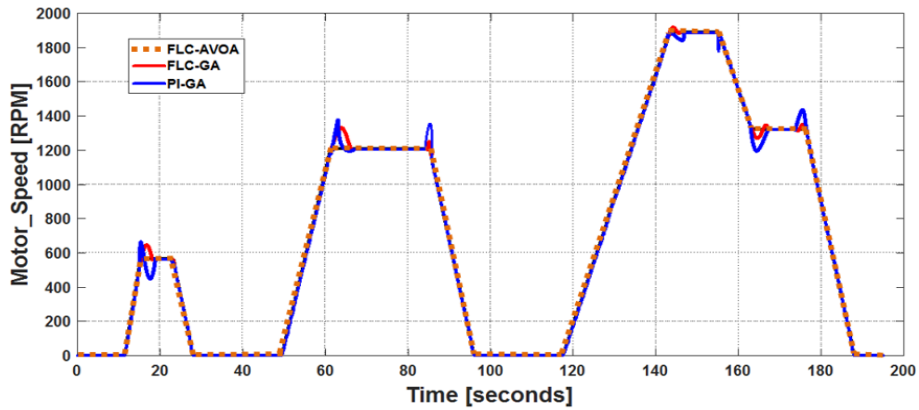


Figure 7. DC motor speed simulation with PI-GA, FLC-GA, and FLC-AVOA

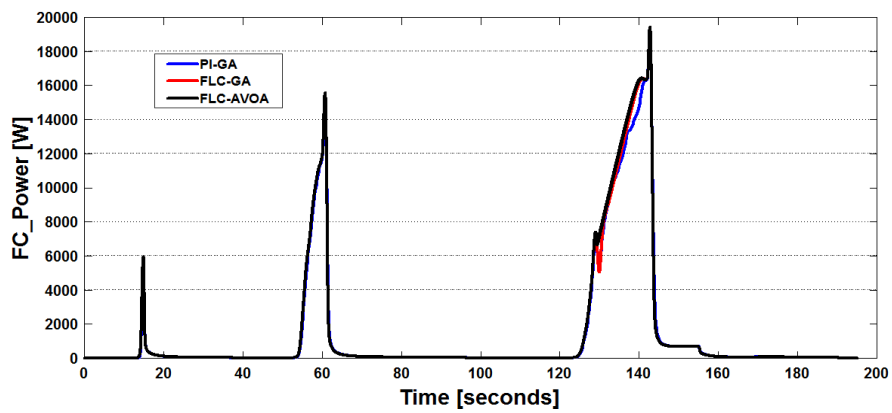


Figure 8. Simulation of Fuel cells power using PI-GA, FLC-GA, and FLC-AVOA

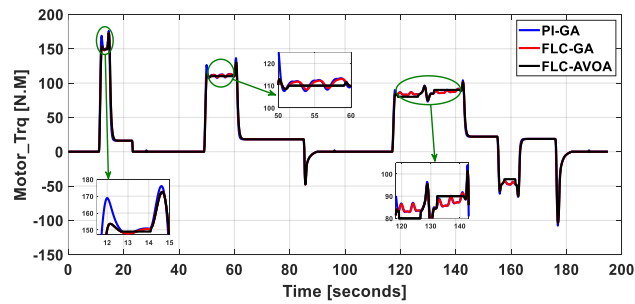


Figure 9. Simulation of the output motor torque of the system using PI-GA, FLC-GA, and FLC-AVOA

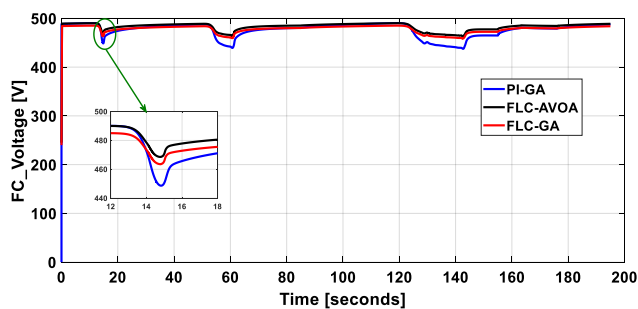


Figure 10. Simulation of the output fuel cell voltage of the system using PI-GA, FLC-GA, and FLC-AVOA




5. CONCLUSION

An FCEV drive system is explored using three distinct control approaches, including a PI speed regulator with GA, a fuzzy logic controller based on GA, and a fuzzy logic controller based on AVOA. The motor speed is controlled by the integral square speed error and its variation. The newly suggested AVOA approach is intriguing owing to its straightforward formulation and ease of implementation. MATLAB/Simulink is used to assess the performance of the induction motor drive system under the researched control techniques. The simulation findings show that employing a fuzzy logic controller in conjunction with the AVOA approach outperforms in terms of dynamic performance. In the fuzzy logic speed regulator, the AVOA reduced the maximum peak overshoot for speed dynamic response by 55.23% and the rising time by 2.31% when compared to GA.




REFERENCES

- [1] R. Yeetsorn and Y. Maiket, "Hydrogen fuel cell implementation for the transportation sector," in *Advanced Applications of Hydrogen and Engineering Systems in the Automotive Industry*, IntechOpen, 2021. doi: 10.5772/intechopen.95291.
- [2] R. Q. Nafil and M. S. Majeed, "Fuel cells as a source of green energy," in *Thermodynamics and Energy Engineering*, IntechOpen, 2020. doi: 10.5772/intechopen.89736.
- [3] T. X. Dinh *et al.*, "Modeling and energy management strategy in energetic macroscopic representation for a fuel cell hybrid electric vehicle," *Journal of Drive and Control*, vol. 16, no. 2, pp. 80–90, 2019, doi: <https://doi.org/10.7839/ksfc.2019.16.2.080>.
- [4] Y. Manoharan *et al.*, "Hydrogen fuel cell vehicles; current status and future prospect," *Applied Sciences*, vol. 9, no. 11, p. 2296, Jun. 2019, doi: 10.3390/app9112296.
- [5] A. S and A. I. Selvakumar, "Modeling and simulation of PEM fuel cell electric vehicle with multiple power sources," *International Journal of Recent Technology and Engineering (IJRTE)*, vol. 8, no. 6, pp. 2967–2975, Mar. 2020, doi: 10.35940/ijrte.F8420.038620.
- [6] T. Selmi, A. Khadhraoui, and A. Cherif, "Fuel cell-based electric vehicles technologies and challenges," *Environmental Science and Pollution Research*, vol. 29, no. 52, pp. 78121–78131, Nov. 2022, doi: 10.1007/s11356-022-23171-w.
- [7] M. İnci, M. Büyüç, M. H. Demir, and G. İlbey, "A review and research on fuel cell electric vehicles: Topologies, power electronic converters, energy management methods, technical challenges, marketing and future aspects," *Renewable and Sustainable Energy Reviews*, vol. 137, p. 110648, Mar. 2021, doi: 10.1016/j.rser.2020.110648.
- [8] D. Mohanraj, J. Gopalakrishnan, B. Chokkalingam, and L. Mihet-Popa, "Critical aspects of electric motor drive controllers and mitigation of torque ripple—review," *IEEE Access*, vol. 10, pp. 73635–73674, 2022, doi: 10.1109/ACCESS.2022.3187515.
- [9] Y. Yu, M. Chen, S. Zaman, S. Xing, M. Wang, and H. Wang, "Thermal management system for liquid-cooling PEMFC stack: From primary configuration to system control strategy," *eTransportation*, vol. 12, p. 100165, May 2022, doi: 10.1016/j.etrans.2022.100165.
- [10] G. A. Ghazi *et al.*, "African vulture optimization algorithm-based PI controllers for performance enhancement of hybrid renewable-energy systems," *Sustainability*, vol. 14, no. 13, p. 8172, Jul. 2022, doi: 10.3390/su14138172.
- [11] M. A. Hannan, F. A. Azidin, and A. Mohamed, "Hybrid electric vehicles and their challenges: A review," *Renewable and Sustainable Energy Reviews*, vol. 29, pp. 135–150, Jan. 2014, doi: 10.1016/j.rser.2013.08.097.
- [12] O. Hegazy and P. Lataire, "Modeling and analysis of different control techniques of electric motor for electric vehicle powertrains," *EPE Journal*, vol. 25, no. 1, pp. 36–46, Mar. 2015, doi: 10.1080/09398368.2015.11782459.
- [13] N. Djararov, "Traction motor drive of electrical vehicle: types, performances and control," in *2022 8th International Conference on Energy Efficiency and Agricultural Engineering (EE&AE)*, Jun. 2022, pp. 1–14. doi: 10.1109/EEAE53789.2022.9831309.
- [14] D. Mohanraj *et al.*, "A review of BLDC motor: State of art, advanced control techniques, and applications," *IEEE Access*, vol. 10, pp. 54833–54869, 2022, doi: 10.1109/ACCESS.2022.3175011.
- [15] U. K. Soni and R. K. Tripathi, "Recent challenges and advances in the sensorless commutation of brushless DC motors," *Recent Advances in Electrical & Electronic Engineering (Formerly Recent Patents on Electrical & Electronic Engineering)*, vol. 14, no. 1, pp. 90–113, Jan. 2021, doi: 10.2174/2352096513999200825105724.
- [16] M. A. Ibrahim, A. N. Hamoodi, and B. M. Salih, "PI controller for DC motor speed realized with simulink and practical measurements," *International Journal of Power Electronics and Drive Systems (IJPEDS)*, vol. 11, no. 1, pp. 119–126, Mar. 2020, doi: 10.11591/ijpeds.v11.i1.pp119-126.
- [17] B. Abdollahzadeh, F. S. Gharehchopogh, and S. Mirjalili, "African vultures optimization algorithm: A new nature-inspired metaheuristic algorithm for global optimization problems," *Computers & Industrial Engineering*, vol. 158, p. 107408, Aug. 2021, doi: 10.1016/j.cie.2021.107408.
- [18] R. H. Mohammed, A. M. Ismaiel, B. E. Elnaghi, and M. E. Dessouki, "African vulture optimizer algorithm based vector control induction motor drive system," *International Journal of Electrical and Computer Engineering (IJECE)*, vol. 13, no. 3, p. 2396, Jun. 2023, doi: 10.11591/ijece.v13i3.pp2396-2408.
- [19] W. Hankache, S. Caux, D. Hissel, and M. Fadel, "Genetic algorithm fuzzy logic energy management strategy for fuel cell hybrid vehicle," *IFAC Proceedings Volumes*, vol. 42, no. 9, pp. 137–142, 2009, doi: 10.3182/20090705-4-SF-2005.00026.
- [20] A. A. Ancaşa and G. Danciu, "Modeling and simulation of an electric propulsion system equipped with Fuel Cell," *IOP Conference Series: Materials Science and Engineering*, vol. 1220, no. 1, p. 012011, Jan. 2022, doi: 10.1088/1757-899X/1220/1/012011.
- [21] U. Usmanov, S. Ruzimov, A. Tonoli, and A. Mukhitdinov, "Modeling, simulation and control strategy optimization of fuel cell hybrid electric vehicle," *Vehicles*, vol. 5, no. 2, pp. 464–481, Apr. 2023, doi: 10.3390/vehicles5020026.
- [22] B. E. Elnaghi, M. N. Abelwhab, A. M. Ismaiel, and R. H. Mohammed, "Solar hydrogen variable speed control of induction motor based on chaotic billiards optimization technique," *Energies*, vol. 16, no. 3, p. 1110, Jan. 2023, doi: 10.3390/en16031110.
- [23] D. Li, F. Gao, Y. Xue, and C. Lu, "Optimization of decentralized PI/PID controllers based on genetic algorithm," *Asian Journal of Control*, vol. 9, no. 3, pp. 306–316, Sep. 2007, doi: 10.1111/j.1934-6093.2007.tb00416.x.
- [24] H. M. Hasanien, "Design optimization of PID controller in automatic voltage regulator system using taguchi combined genetic algorithm method," *IEEE Systems Journal*, vol. 7, no. 4, pp. 825–831, Dec. 2013, doi: 10.1109/JSYST.2012.2219912.
- [25] M. Essoufi, B. Hajji, and A. Rabhi, "Fuzzy logic based energy management strategy for fuel cell hybrid electric vehicle," in *2020 International Conference on Electrical and Information Technologies (ICEIT)*, Mar. 2020, pp. 1–7. doi: 10.1109/ICEIT48248.2020.9113162.




BIOGRAPHIES OF AUTHORS

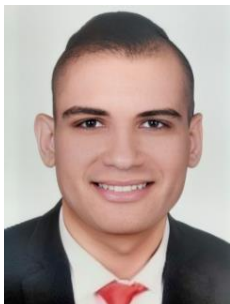
Basem E. Elnaghi    graduated from Suez Canal University in Port Said, Egypt, in 2002 with a B.Sc., M.Sc., and Ph.D. in electrical power engineering. He has been an associate professor in the Suez Canal University College of Engineering's Electrical Engineering Department since 2015. He became a member of the Engineering Department at Suez Canal University. His primary areas of interest in the workplace include power electronics applications, control of electrical machines and wind energy conversion systems, direct torque and field-oriented control approaches, DSP control, and AC and DC drives. He can be contacted at email: Basem_elhady@eng.suez.edu.eg.






Mohammed Elshahat Dessouki    was born in Bohiera, Egypt in 1976. He received his B.Sc., M.Sc., and Ph.D. degrees, from Faculty of Engineering, Suez Canal University in 1999, 2004, and 2010, respectively, all in Electrical Engineering. He joined the Department of Electrical Engineering, Faculty of Engineering, Suez Canal University as a demonstrator in 2000. Then, he became an assistant lecturer from 2004 to 2010 and has been a lecturer since 2010. He joined the Department of Electrical Engineering, King Abdulaziz University, in Rabigh. His main professional interests include AC and DC drives, direct torque and field-oriented control techniques, and DSP control and power electronics applications. He can be contacted at email: dessouky_m@yahoo.com.






Sarah Wahied Mohamed    was born on July 2, 1993. She received the B.Sc. degrees from higher technological institute in 2016. Currently, she works as technical office and production engineer at Elsewedy Factory, Cairo, Egypt. She is interested in electric panel, automation control, renewable energy, motor drive design, and power electronics applications. She can be contacted at email: sarah.wahied1@gmail.com.



Ahmed M. Ismaiel    was born on September 19, 1996. He obtained his B.Sc. and M.Sc. degrees from the faculty of engineering at Suez Canal University in 2019 and 2021, respectively. He is currently employed as an assistant lecturer in the Electrical Power and Machine Engineering Department at Suez Canal University in Ismailia, Egypt. He is interested in automation control, renewable energy, motor drive design and vector control approaches, as well as DSP control, and power electronics applications. He can be contacted at email: ahmed123ismaiel@gmail.com.



Mohamed Nabil Abdel-Wahab    received his B.Sc. from Zagazig University, followed by his M.Sc. and Ph.D. from Mansoura University. He served as a super-intended engineer in (Naval Medical Research Unit) NAMRU-3 in Cairo, then as an external electrical officer engineer in rebuilding the electrical network of Abu Hamad Air Base, before moving to Egyptian Electricity Transmission Company (EETC) as a consultant engineer. Dr. M.N. Abdel-Wahab was eventually hired as an assistant professor (teaching staff member) in the Electrical Engineering Department of the Faculty of Engineering at Suez Canal University. He has thirty papers published in international publications and in national and international conferences. He can be contacted at email: mohamed.nabil@eng.suez.edu.eg.